organic compounds

DL-Proline

Sunnie Myung, Maren Pink,* Mu-Hyun Baik and David E. Clemmer

Department of Chemistry, Indiana University, 800 E. Kirkwood, Bloomington, IN 47405, USA
Correspondence e-mail: mpink@indiana.edu

In the structure of DL-proline, $C_5H_9NO_2$, the molecules are connected via classical intermolecular N—H···O hydrogen bonds involving the amine and carboxyl groups [N···O = 2.7129 (15) and 2.8392 (16) Å], and form chains along the b-axis direction and parallel to ($\bar{1}$01). The chains are linked into sheets via weak non-classical hydrogen bonds. The conformation of the molecule and its packing are notably different from the monohydrated DL-proline form.

Comment

Structural data for amino acids are fundamentally important. Aside from recent electron-density studies (Flaig et al., 2002; Abramov et al., 2000) and quantum chemical investigations (Brauer et al., 2004; Czinki & Császár, 2003; Stepanian et al., 2001; Improta et al., 2001), the study of amino acid clusters in the gas phase has attracted considerable attention (Cooks et al., 2001; Julian et al., 2002; Counterman & Clemmer, 2001; Myung et al., 2004). Although the majority of amino acids have been crystallized as enantiopure L and racemic DL forms and their structures are known, a few remain elusive, notably DL-proline, (I).
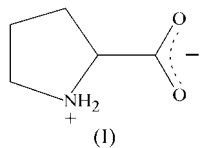
Proline is an abundant amino acid in collagen and is exceptional among the amino acids; it is the only one in which the amine group is part of a pyrrolidine ring, making it rigid and directional in biological systems despite its conformational flexibility. So far, the crystal structures of L-proline (Kayushina & Vainshtein, 1965), the monohydrates of L- and DL-proline [Janczak & Luger (1997) and Padmanabhan et al. (1995), respectively], and numerous other solvates and salts of proline have been determined. We report here the crystal structure of DL-proline (Fig. 1).

DL-Proline crystallizes in its zwitterionic form with long C—N bond lengths [1.4907 (18) and 1.5104 (19) Å; Table 1] and a slightly asymmetrical carboxyl group [C—O = 1.2733 (17) and 1.2387 (18) Å]. The pyrrolidine ring adopts a C_2—C^γ-endo conformation (Ashida & Kakudo, 1974) similar to that of L-proline (Kayushina & Vainshtein, 1965). Atom C4 (or C^γ) is located 0.988 (3) Å above the N1/C2/C3 (or $N/C^\alpha/C^\beta$) plane. The angle between atom C1 and the N1/C2/C3 plane is 126.0 (4)°. The ring puckering parameters (Cremer & Pople, 1975) for the pyrrolidine ring are $q_2 = 0.4029$ (16) Å and $\varphi_2 = 57.7$ (2)°. For comparison, the puckering parameters of L-proline are $q_2 = 0.404$ Å and $\varphi_2 = 89.1$°. In contrast, the puckering parameters for the monohydrates are $q_2 = 0.4033$ (5) Å and $\varphi_2 = 308.63$ (7)°, and $q_2 = 0.395$ (4) Å and $\varphi_2 = 309.9$ (6)° for the DL and L forms, respectively.

Classical hydrogen bonds between carboxyl and ammonium ion groups link the molecules into chains (Table 2 and Fig. 2) parallel to ($\bar{1}$01), that can be described by the first level graph sets $C(5)$ and $R_2^2(10)$ and the second level graph set $R_4^2(8)$ (Etter et al., 1990). Interestingly, only one of the carboxyl O atoms (O1), showing a slightly elongated C—O distance, is involved in classical hydrogen bonding. The second O atom (O2) is surrounded by aliphatic H atoms at distances greater than 2.6 Å. Considering the rather long distances, both O atoms form non-classical hydrogen bonds to C atoms; these bonds group the hydrogen-bonded chains into slip-stacked
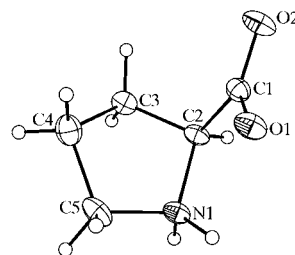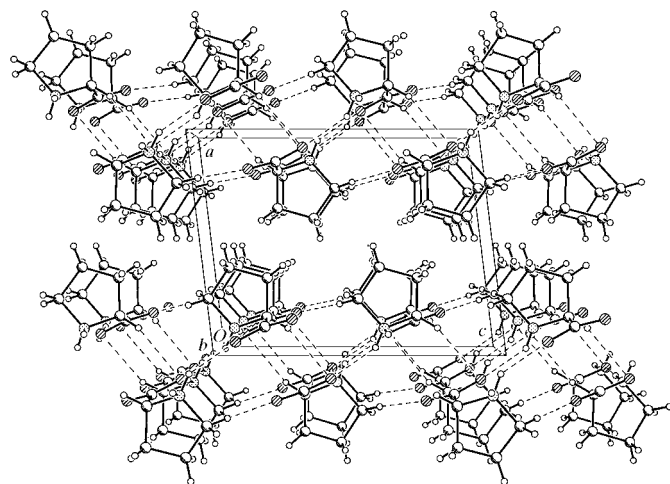

Figure 1
A view of DL-proline with the atom-labeling scheme. Displacement ellipsoids are drawn at the 50% probability level, with H atoms represented by circles of arbitrary size.
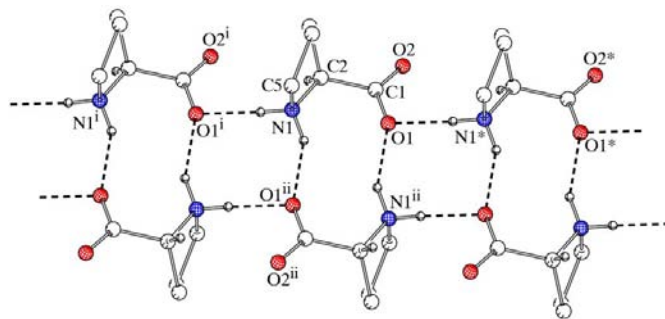
Figure 2
The hydrogen-bonding pattern along (010), with chains parallel to ($\bar{1}$01). The secondary CH$_2$ H atoms have been omitted for clarity. Symmetry codes are as in Table 2; atoms marked with an asterisk (*) are at (x, 1 + y, z).

layers parallel to (100), with the hydrophobic regions of the layers facing each other (Fig. 3). For comparison, in both L- and DL-proline monohydrate, the molecules are linked into three-dimensional hydrogen-bonded networks that include the water molecules in channels. In L-proline, the molecules form sheets *via* hydrogen bonding, with both carboxyl O atoms participating in the N—H···O interaction.

The study of conformational differences of proline is of interest because of its importance in collagen (DeRider *et al.*, 2002). To achieve a general understanding of proline's conformational flexibility, we carried out DFT-based (DFT is density functional theory) geometry optimizations. Crystallographic data available for L-proline (Kayushina & Vainshtein, 1965), the monohydrates of L- and DL-proline (Janczak & Luger, 1997; Padmanabhan *et al.*, 1995), and our own results provided initial geometries. Not surprisingly, standard gas phase calculations indicate that in all cases the zwitterionic form of proline is not a well defined minimum on the gas phase molecular potential energy surface. As expected, all geometry optimizations converged to a neutral form. The zwitterionic structures could be optimized successfully, however, by including a continuum field in the computation of the gradient, which, one could argue, mimics the environment in a crystal or protein. The COSMO method was used (Klamt & Schüürmann, 1993), which was originally designed to mimic charge screening due to solvent. As COSMO, like any other continuum solvation method, simply simulates the response of a dielectric continuum to the charge density of the solute, it is reasonable to make use of this protocol for simulating the effects of the electrostatic response potential present in the proline crystal. Since continuum models use a simple scaling factor to account for different dielectric constants, the potential energy surface does not change its shape as a function of the dielectric constant. Thus, for the purpose of obtaining the geometry of a proline molecule embedded in the

continuum potential and evaluating the relative energies of different conformers, the choice of the actual parameter for the dielectric constant is not physically relevant. We used the dielectric constant of water ($\varepsilon = 78.4$) because the continuum models are best calibrated to this dielectric constant.

The geometry optimizations gave rise to only small adjustments of the different X-ray structures. Both *endo* and *exo* conformers of the zwitterionic proline are obtained as stable structures, and conformations were maintained for unsolvated and monohydrated prolines, respectively. The energies of the four different structures with and without the COSMO potential [E(COSMO) and E(GP), respectively] are listed in Table 3. Interestingly, the *endo* and *exo* conformers are practically isoenergetic when the continuum potential is included, the computed energy difference being 0.7 kcal mol^{-1} at best. However, the gas phase energies E(GP) evaluated at the same geometry reveal that there is a slight electronic preference of 2 kcal mol^{-1} for the *endo* conformer.

Experimental

Compound (I) was recrystallized by slow evaporation from a concentrated solution in dry methanol (Aldrich) using commercially available material [Aldrich, m.p. 481 (3) K]. All calculations were carried out using density functional theory (Parr & Yang, 1989; Ziegler, 1991) as implemented in the Amsterdam Density Functional 2004.01 package (*ADF*; Velde *et al.*, 2001), using a triple-z STO basis set with one set of polarization functions as provided in the *ADF* package (basis set TZP), together with the BLYP functional (Becke, 1988; Lee *et al.*, 1988). The COSMO potential (Pye & Ziegler, 1999) was included in the SCF procedure and the following radii were used to obtain the solute cavity: C 1.9 Å, O 1.6 Å, N 1.6 Å, H 1.15 Å. The dielectric constant ε was set at 78.4. All calculations were carried out using the restricted spin formalism (closed-shell).

Figure 3
The molecular packing of DL-proline, viewed along the *b* axis. Dashed lines show classical and non-classical hydrogen bonding.

Crystal data

C₅H₉NO₂	$D_x = 1.409$ Mg m^{-3}
$M_r = 115.13$	Mo $K\alpha$ radiation
Monoclinic, $P2_1/c$	Cell parameters from 1925
$a = 8.9906$ (6) Å	reflections
$b = 5.2987$ (4) Å	$\theta = 2.3–50.0°$
$c = 11.4786$ (8) Å	$\mu = 0.11$ mm^{-1}
$\beta = 97.041$ (2)°	$T = 120$ (2) K
$V = 542.70$ (7) Å^3	Block, colorless
$Z = 4$	$0.24 \times 0.11 \times 0.10$ mm

Data collection

Bruker SMART 6000	963 independent reflections
diffractometer	855 reflections with $I > 2\sigma(I)$
ω scans	$R_{int} = 0.021$
Absorption correction: multi-scan	$\theta_{max} = 25.0°$
(*SADABS*; Blessing, 1995)	$h = -10 \rightarrow 10$
$T_{min} = 0.974$, $T_{max} = 0.990$	$k = -6 \rightarrow 5$
3327 measured reflections	$l = -13 \rightarrow 12$

Refinement

Refinement on F^2	$w = 1/[\sigma^2(F_o^2) + (0.0745P)^2$
$R[F^2 > 2\sigma(F^2)] = 0.040$	$+ 0.1713P]$
$wR(F^2) = 0.114$	where $P = (F_o^2 + 2F_c^2)/3$
$S = 1.06$	$(\Delta/\sigma)_{max} < 0.001$
963 reflections	$\Delta\rho_{max} = 0.37$ e Å^{-3}
87 parameters	$\Delta\rho_{min} = -0.19$ e Å^{-3}
H atoms treated by a mixture of	
independent and constrained	
refinement	

organic compounds

Table 1
Selected geometric parameters (Å, °).

C1—O2	1.2387 (18)	N1—C2	1.4907 (18)
C1—O1	1.2733 (17)	N1—C5	1.5104 (19)
C1—C2	1.5361 (19)		
O2—C1—O1	126.79 (13)	N1—C2—C3	102.25 (11)
O2—C1—C2	116.66 (12)	N1—C2—C1	111.08 (11)
O1—C1—C2	116.55 (12)	N1—C5—C4	105.18 (11)
C2—N1—C5	107.78 (11)		
O2—C1—C2—N1	178.49 (12)	O2—C1—C2—C3	−67.73 (16)
O1—C1—C2—N1	−1.34 (17)	O1—C1—C2—C3	112.44 (13)

Table 2
Hydrogen-bond geometry (Å, °).

D—H···A	D—H	H···A	D···A	D—H···A
N1—H1N···O1^{i}	0.92 (2)	1.80 (2)	2.7129 (15)	172 (2)
N1—H1M···O1^{ii}	0.90 (2)	2.09 (2)	2.8392 (16)	139 (2)
C2—H2···O1^{iii}	1.00	2.58	3.4857 (17)	151
C5—H5A···O2^{iv}	0.99	2.69	3.6759 (18)	173

Symmetry codes: (i) $x, y − 1, z$; (ii) $−x, −y + 1, −z$; (iii) $−x, y − \frac{1}{2}, −z + \frac{1}{2}$; (iv) $x, −y + \frac{3}{2}, z − \frac{1}{2}$.

Table 3
Computed electronic energies and energy differences with and without the COSMO potential switched on at the COSMO-optimized geometries.

Molecule	$E(COSMO)^{a}$	$\Delta E(COSMO)^{b}$	$E(GP)^{a}$	$\Delta E(GP)^{b}$
DL-Proline	−103.1375	0	−101.5864	0
L-Proline	−103.1364	0.02	−101.5846	0.04
DL-Proline hydrate	−103.1159	0.50	−101.5123	1.71
L-Proline hydrate	−103.1081	0.68	−101.4970	2.06

Units: (a) eV; (b) kcal mol^{-1}.

H atoms participating in classical hydrogen bonding were located in a difference map and refined. All other H atoms were placed in idealized positions, with C—H distances of 0.99 Å for the secondary (CH$_2$) groups and 1.00 Å for the tertiary (CH) group. H atoms were treated using a riding model with individual refined displacement parameters for all H atoms apart from H2, for which the U_{iso}(H) value was fixed at $1.2U_{eq}$ of the parent C2 atom. The residual electron density is small, with the highest peak located on the C2–C3 bond. Additional peaks are located in the vicinity of the O atoms and on bonds.

Data collection: *SMART* (Bruker, 2001); cell refinement: *SAINT* (Bruker, 2003); data reduction: *SAINT*; program(s) used to solve structure: *SHELXS97* (Sheldrick, 1990); program(s) used to refine structure: *SHELXL97* (Sheldrick, 1997); molecular graphics: *SHELXTL* (Bruker, 2003), *XTEL* (local library) and *PLATON* (Spek, 2002); software used to prepare material for publication: *SHELXTL*.

References

Abramov, Y. A., Volkov, A., Wu, G. & Coppens, P. (2000). *J. Phys. Chem. B*, **104**, 2183–2188.
Ashida, T. & Kakudo, M. (1974). *Bull. Chem. Soc. Jpn*, **47**, 1129–1133.
Becke, A. D. (1988). *Phys. Rev. A*, **38**, 3098–3100.
Blessing, R. H. (1995). *Acta Cryst.* A**51**, 33–38.
Brauer, B., Chaban, G. M. & Gerber, R. B. (2004). *Phys. Chem. Chem. Phys.* **6**, 2543–2556.
Bruker (2001). *SMART*. Bruker AXS Inc., Madison, Wisconsin, USA.
Bruker (2003). *SAINT* and *SHELXTL*. Bruker AXS Inc., Madison, Wisconsin, USA.
Cooks, G. R., Zhang, D., Koch, K. J., Gozzo, F. C. & Eberlin, M. N. (2001). *Anal. Chem.* **73**, 3646–3655.
Counterman, A. E. & Clemmer, D. E. (2001). *J. Phys. Chem. B*, **105**, 8092–8096.
Cremer, D. & Pople, J. A. (1975). *J. Am. Chem. Soc.* **97**, 1354–1358.
Czinki, E. & Császár, A. G. (2003). *Chem. Eur. J.* **9**, 1008–1019.
DeRider, M. L., Wilkens, S. J., Waddell, M. J., Bretscher, L. E., Weinhold, F., Raines, R. T. & Markley, J. J. (2002). *J. Am. Chem. Soc.* **124**, 2497–2505.
Etter, M. C., MacDonald, J. C. & Bernstein, J. (1990). *Acta Cryst.* B**46**, 256–262.
Flaig, R., Koritsanszki, T., Dittrich, B., Wagner, A. & Luger, P. (2002). *J. Am. Chem. Soc.* **124**, 3407–3417.
Improta, R., Benzi, C. & Barone, V. (2001). *J. Am. Chem. Soc.* **123**, 12568–12577.
Janczak, J. & Luger, P. (1997). *Acta Cryst.* C**53**, 1954–1956.
Julian, R. R., Hodyss, R., Kinnear, B., Jarrold, M. F. & Beauchamp, J. L. (2002). *J. Phys. Chem. B*, **106**, 1219–1228.
Kayushina, R. L. & Vainshtein, B. K. (1965). *Kristallografiya*, **10**, 833–844.
Klamt, A. & Schüürmann, G. (1993). *J. Chem. Soc. Perkin Trans. 2*, pp. 799–805.
Lee, C. T., Yang, W. T. & Parr, R. G. (1988). *Phys. Rev. B*, **37**, 785–789.
Myung, S., Julian, R. R., Nantia, S. C., Cooks, R. G. & Clemmer, D. E. (2004). *J. Phys. Chem. B*, **108**, 6105–6111.
Padmanabhan, S., Suresh, S. & Vijayan, M. (1995). *Acta Cryst.* C**51**, 2098–2100.
Parr, R. G. & Yang, W. (1989). *Density Functional Theory of Atoms and Molecules*. New York: Oxford University Press.
Pye, C. C. & Ziegler, T. (1999). *Theor. Chem. Acc.* **101**, 396–408.
Sheldrick, G. M. (1990). *Acta Cryst.* A**46**, 467–473.
Sheldrick, G. M. (1997). *SHELXL97*. University of Göttingen, Germany.
Spek, A. L. (2002). *PLATON*. University of Utrecht, The Netherlands.
Stepanian, S. G., Reva, I. D., Radchenko, E. D. & Adamowicz, L. (2001). *J. Phys. Chem. A*, **105**, 10664–10672.
Velde, G. T., Bickelhaupt, F. M., Baerends, E. J., Guerra, C. F., Van Gisbergen, S. J. A., Snijders, J. G. & Ziegler, T. (2001). *J. Comput. Chem.* **22**, 931–967.
Ziegler, T. (1991). *Chem. Rev.* **91**, 651–667.